Energetics driving the short-range order in Cu_xPd_{1-x}/Ru(0001) monolayer surface alloys†‡

A. Bergbreiter,[a] H. E. Hoster,*[a] S. Sakong,§[b] A. Groß[b] and R. J. Behm*[a]

Received 5th April 2007, Accepted 13th July 2007
First published as an Advance Article on the web 31st July 2007
DOI: 10.1039/b705237p

The energetics determining the distinct short-range order in two-dimensional (2D) monolayer Cu_xPd_{1-x} surface alloys on a Ru(0001) substrate were investigated by Monte Carlo simulations and density functional theory calculations. Using a 2D lattice gas Hamiltonian based on effective pair interaction (EPI) parameters, the EPIs were derived for different Cu concentrations with Monte Carlo (MC) simulations by comparing with the atomic distributions obtained from atomic resolution STM images and the related Warren–Cowley short-range order parameters (Hoster *et al.*, *Phys. Rev. B*, 2006, **73** 165413). The ground state structures and mixing energies at 0 K derived from these EPIs agree well with mixing energies determined from DFT calculations of different ordered surface alloys. Additional MC simulations yield rather low transition temperatures which explain the absence of ordered 2D phases in the experiments. The consequences of our findings for the use of alloy surfaces and surface alloys as model systems for adsorption and catalytic reaction studies are discussed.

1. Introduction

Bimetallic surface alloys have attracted considerable interest recently as model systems for studying the physical and chemical properties of bimetallic systems under well-defined conditions and, because of the limitation to two dimensions (2D), in a simplified configuration.[1–4] Features of interest included the formation of bulk immiscible 2D alloy phases,[5–9] 2D phase diagrams and phase transitions in the alloy layer and the underlying interactions between the surface atoms,[3,10–12] 2D intermixing kinetics or the dependence of the adsorption and reaction behavior on the concentration and lateral distribution of the two components in order to elucidate the role of specific atomic configurations in these processes,[13–15] as they had been proposed earlier (ensemble effect, ligand effect[16,17]). Pre-eminent for the further progress in these topics is a quantitative knowledge of the surface composition and of the distribution of the respective components in the surface layer. This information can be provided by systematic, high-resolution scanning tunneling microscopy studies, characterizing the distribution of surface atoms in surface layers with different concentrations of the components by atomic resolution scanning tunneling microscopy (STM) imaging with chemical contrast,[9,13,18–23] and a quantitative evaluation and description of the atomic arrangement, *e.g.*, by the Warren–Cowley short-range order parameters (see below).

The distribution of surface atoms in the 2D surface alloy is, at least under conditions at or close to equilibrium, dominated by the interactions between the respective surface species. This is the topic of the present contribution, which describes the determination of the interaction energies between the two components Cu and Pd in Cu_xPd_{1-x} monolayer surface alloys on Ru(0001) by Monte Carlo simulations and density functional theory calculations. As part of an ongoing long-term study on the structure and reactivity of bimetallic surface alloys,[13,15,20,22,24–29] the distribution of the respective components in these Cu_xPd_{1-x} monolayer surface alloys was recently characterized by high resolution STM imaging[26] and related to the CO adsorption characteristics.[25,27] Although long-range ordered structures were not observed, the 2D alloys exhibit a characteristic short-range order (SRO) with a preference for dissimilar neighbors. In analogy to the formalism used in studies of bulk alloys,[30–32] the energy of a given atomic distribution can be described by a 2D lattice gas Hamiltonian of the form $H = \frac{1}{2}\sum_{i,j} V_{ij}S_iS_j$,[11–12,33,34] if only pairwise interactions are considered. S_i and S_j represent the atom types at sites i and j, respectively, and can take the values $+1$ and -1. The effective pair interaction (EPI) parameters V_{ij} only depend on the distance between the sites i and j and describe the energetic difference between like and unlike pairs of neighbors on sites i and j. For a 2D lattice containing atom types A and B, V_{ij} is related to the interaction potentials V_{ij}^{AA}, V_{ij}^{BB}, and V_{ij}^{AB} *via* the equation $V_{ij} = \frac{1}{2}(V_{ij}^{AA} + V_{ij}^{BB} - 2V_{ij}^{AB})$.[11] V_{ij} turns positive or negative if either unlike or like pairs are energetically favorable, respectively, for a given interatomic distance between i and j. From a given atomic distribution, only the term V_{ij} can be derived while the individual interactions contributing to this parameter are not accessible. In the following, we replaced

[a] *Institute of Surface Chemistry and Catalysis, Ulm University, D-89069 Ulm, Germany. E-mail: harry.hoster@uni-ulm.de, juergen.behm@uni-ulm.de*
[b] *Institute of Theoretical Chemistry, Ulm University, D-89069 Ulm, Germany*
† The HTML version of this article has been enhanced with colour images.
‡ This paper was submitted as part of the special issue 'Bridging the pressure and material gap in heterogeneous catalysis'.
§ Present address: Department of Physics, University Duisburg-Essen, D-47048, Duisburg, Germany

the indices i and j denoting the lattice sites by the distance r between the respective lattice sites. An atomic distribution governed by a given set of EPIs can be generated *via* a Metropolis Monte-Carlo (MC) algorithm in which temperature effects are also included.[35,36]

In the present study, we derived the EPIs dominating the short-range order in 2D Cu_xPd_{1-x}/Ru(0001) monolayer surface alloys by a systematic search based on Monte-Carlo simulations, which basically involves a systematic variation of the EPI parameter set, minimizing the mean square difference between the SRO parameters of the atomic distributions derived from the STM images and the MC-generated atomic distributions, similar to an analysis performed previously by Sadigh *et al*. for PdAu/Ru(0001) surface alloys.[33] Although the measured atomic distributions are representative for temperatures around 600 K, which are necessary for 2D intermixing, the resulting EPIs allow for the determination of the ordered $T = 0$ K ground-state structures at the given compositions and of the transition temperature T_c, below which the formation of such ordered structures can be expected at all.

After a brief summary of our experimental and computational methods, an overview of the EPI parameters derived from the experimentally determined atomic distributions[26] and the MC simulated SROs is given. Based on these data, we calculated the energies of different ordered ground state structures. For some ordered surface alloy structures, mixing enthalpies derived from the EPI parameters are compared with the corresponding results obtained from density functional theory (DFT) calculations. We then discuss the thermodynamic stability of distinct long-range ordered 2D structures and estimate the corresponding order–disorder transition temperatures T_c on the basis of MC simulations. The results are compared with data reported for (i) Cu_xPd_{1-x} bulk alloys,[31,32] (ii) Cu_xPd_{1-x}/Cu(111) surface alloys,[34] and (iii) 2D Pd_xAu_{1-x}/Ru(0001) alloys.[33] Finally, we briefly discuss the consequences of these results for the use of surface alloys as model systems in adsorption and reaction studies

2. Methods

Details about the experimental set-up and the experimental procedures for preparing the 2D surface alloys were given elsewhere,[26] together with representative STM images. Due to the high affinity of both metals to the Ru(0001) substrate pseudomorphic and atomically well-dispersed 2D Cu_xPd_{1-x} adlayers are easily formed by sequential deposition of the two components Cu and Pd (total coverage about 1 monolayer), followed by brief annealing (30 s) to 780 K. This temperature was tested to provide sufficient mobility for diffusion and intermixing in the CuPd surface layer, while the incorporation of Cu or Pd into the Ru substrate was found to be negligible.[26] The atomic distributions as measured by STM at 300 K will actually reflect the distribution at 600 K during the cooling process, which was found to be the onset temperature for 2D intermixing of separated Cu and Pd adlayers on Ru(0001).[26] The STM images, which in total contained more than 60 000 atoms, were transformed into hexagonally packed 'maps' for statistical evaluation. The MC simulations of the atomic distributions were performed based on the Metropolis algorithm,[35] assuming a temperature of 600 K. For each experimentally found distribution, the best set of EPIs was determined *via* a simplex downhill algorithm,[37,38] using the EPIs $V(r)$ ($r = 1, \sqrt{3}, 2, \sqrt{7}, 3$) as variables and aiming at a maximum agreement between MC-generated and measured SROs and Warren–Cowley SRO parameters $\alpha_{AB}(r)$. The latter were calculated from the STM data *via* the equation $\alpha_{AB}(r) = 1 - \frac{p_{AB}(r)}{x_B}$.[33,39,40] Here, the probability to find an atom B at a distance r from an atom A is described by the parameter $p_{AB}(r)$, while x_B denotes the fraction of type B atoms in the surface layer. For random alloys $p_{AB}(r)$ and x_B have identical values, resulting in a SRO parameter $\alpha_{AB}(r)$ of zero. In the surface layer, r takes the values of 1, $\sqrt{3}$, 2, $\sqrt{7}$, or 3 nearest-neighbor distances. Maximum agreement between measured and simulated distribution is equivalent to a minimum of the parameter Δ defined by the relation $\Delta = \sum_{r=1,\sqrt{3},2,\sqrt{7},3} (p_{AB}^{exp}(r) - p_{AB}^{MC}(r))^2$. The energies of ordered structures ($T = 0$ K) can be calculated directly from the EPIs.

Density functional theory (DFT) calculations were performed using the Vienna *ab initio* simulation package (VASP).[41] The exchange–correlation effects are described within the generalized gradient approximation (GGA) using the RBPE functional.[42] The ionic cores are represented by the projector augmented wave (PAW) method.[43,44] The electronic wave functions are expanded in a plane wave basis set with an energy cut-off of 400 eV. The surface alloys are represented by Cu, Pd or Cu_xPd_{1-x} monolayers on top of Ru(0001) slabs with a thickness of five layers. The overlayers as well as the two underlying Ru layers are fully relaxed, vertically and laterally. Depending on the Cu : Pd-ratio, ($\sqrt{3} \times \sqrt{3}$), (2×2), or (2×1) unit cells were used. The relative error in the mixing enthalpies derived from the DFT total energies is estimated to be of the order of ± 10 meV.

The energies of all structures in this paper are given in eV or meV per surface atom, and all 2D mixing energies refer to an equilibrium between an intermixed CuPd/Ru(0001) adlayer on the one hand and pseudomorphic Cu/Ru(0001) and Pd/Ru(0001) adlayers on the other hand.

3. Results and discussion

EPI parameters

The STM data revealing the atomic distribution in the Cu_xPd_{1-x}/Ru(0001) 2D alloys and SRO parameters derived from these distributions were presented in a previous publication.[26] Fig. 1a shows the EPI's $V(r)$ derived from these data for a number of Cu : Pd ratios, with r reaching from 1 to 3 nearest neighbor (NN) distances in the surface, *i.e*., up to the 5th shell. Fig. 1b presents the same data plotted as a function of the Cu content. The error bars reflect the range in which each EPI could be varied independently while keeping the MC generated SRO in sufficient agreement with the measured one. As a necessary condition for sufficient agreement we defined that the largest of the average differences between measured and simulated SRO parameters is still smaller than twice the standard deviation of the corresponding simulated parameter.

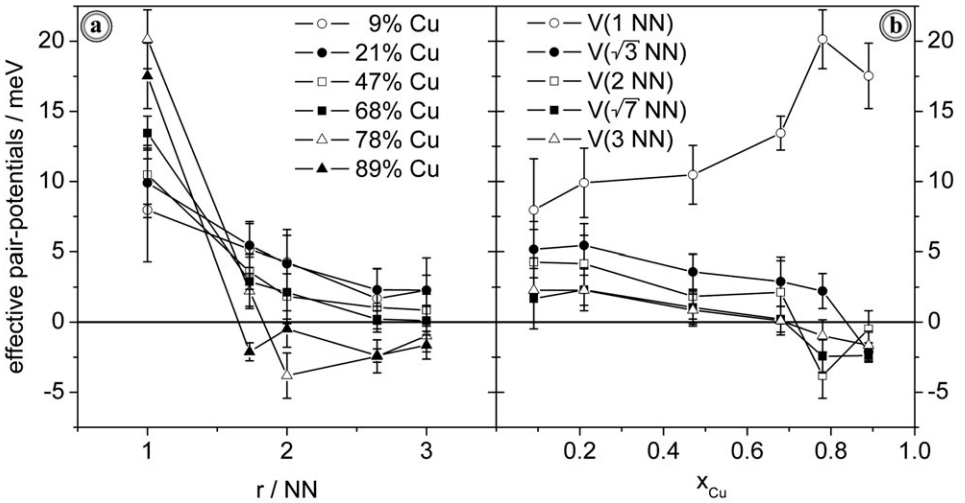

Fig. 1 Overview of the effective pair-potentials $V(r)$ plotted (a) for each x_{Cu} as function of r, with r given as multiples of the nearest-neighbor distances, and (b) for each r as function of Cu content.

The average difference and the standard deviation result from 20 MC generated distributions simulated for a given set of EPIs.

The energetic preference for unlike neighbors, which is the dominating feature in the SRO,[26] is reflected by a large positive value of $V(1)$, in agreement with the behavior of Cu_xPd_{1-x} bulk alloys.[32] For $x_{Cu}<0.7$, also the EPIs for the more remote spheres are positive, while for higher Cu contents we find negative values of $V(r)$ for larger r values. An excellent agreement between the MC simulated and the experimentally found[26] atomic distribution, as is apparent in the quantitative comparison of the respective SRO parameters shown in Fig. 2, confirms that the EPIs are a suitable parametrization of the energetic behavior of the CuPd 2D alloys. The parameters exhibit, however, a non-negligible composition dependence: For instance, for composition independent EPIs, the SROs of $x_{Cu} = 0.22$ and $x_{Cu} = 0.78$ would be identical, in contrast to the experimental findings (*cf.*, Fig. 2). Most directly, the effect of the Pd : Cu ratio can be related to the increasing strain effects in the bimetallic surface layer with increasing Pd contents (for $x < 0.24$) or increasing Cu content ($x > 0.24$, see next paragraph), but other (electronic) effects can not be excluded from the present data.

Ground state structures and order–disorder transitions

The EPIs also determine the thermodynamics of the 2D Cu_xPd_{1-x} alloys at lower temperatures, including the $T = 0$ ground state structures. These are identified by simulated 'annealing' procedures, simulating the atomic distribution at stepwise lowered temperature as successfully performed for Cu_xPd_{1-x} bulk alloys.[32] For ordered structures, the 2D mixing energy per atom can be calculated as the weighted sum of the respective EPIs, with the weighting coefficients reflecting the frequency of their appearance in the unit cell, minus the interaction energies of the pure 2D phases.

The mixing energy itself denotes the energy gain per atom with respect to the stoichiometrically weighted sum of the energies of separated pseudomorphic Cu/Ru(0001) and Pd/Ru(0001) adlayers.[11] Fig. 3 gives an overview of the mixing energy per atom for a large number of different ordered structures. As EPI parameters for a given coverage we used those derived from the STM data set with a Cu : Pd-ratio as close as possible to the desired one. The error bars reflect the variations in the mixing energy associated with the uncertainty of the EPIs as indicated by the error bars in Fig. 1. Specifically, the mixing energy was calculated for each set of EPIs yielding a simulated SRO sufficiently close to the measured one, and

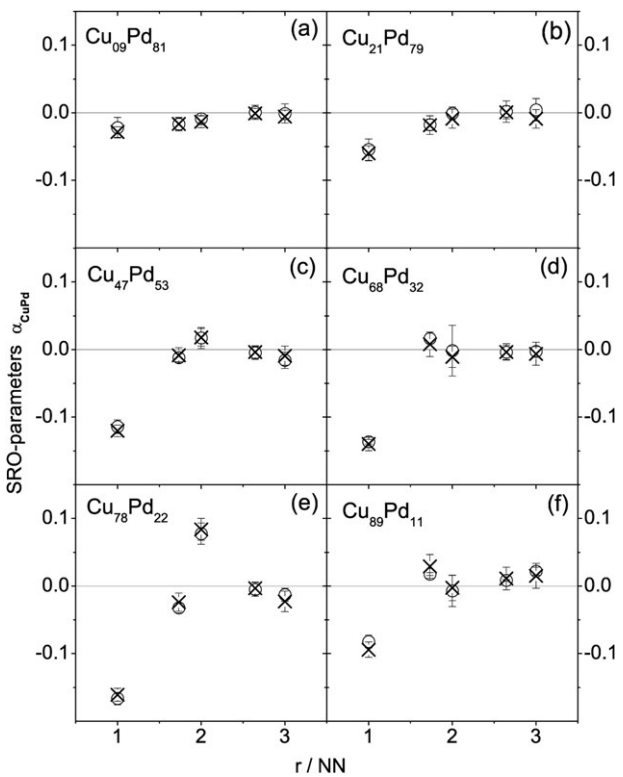

Fig. 2 Comparison of Warren–Cowley SRO parameters determined from experimental data (○) and from MC simulations (×) at different compositions of the Cu_xPd_{1-x} layer. (a) $Cu_{09}Pd_{91}$, (b) $Cu_{21}Pd_{79}$, (c) $Cu_{47}Pd_{53}$, (d) $Cu_{68}Pd_{32}$, (e) $Cu_{78}Pd_{21}$, (f) $Cu_{89}Pd_{11}$.

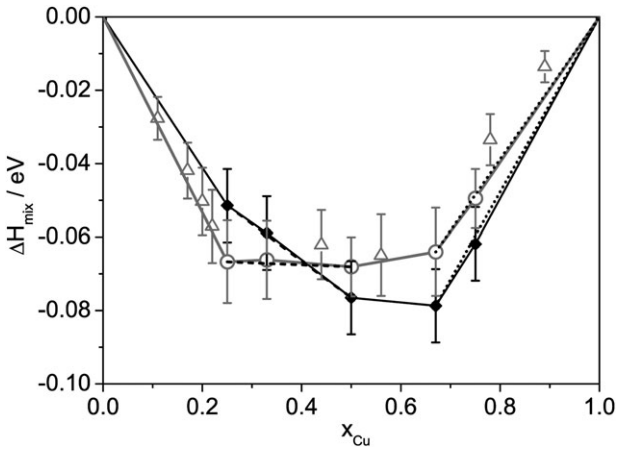

Fig. 3 Mixing enthalpies at $T = 0$ K for selected Cu : Pd ratios. (○) Ordered ground state structures according to the experimentally derived effective pair interactions; (♦) corresponding DFT results; (△) ordered structures with lowest energy, but unstable against phase separation into neighboring ground state structures.

the error bars in Fig. 3 reflect the range of values attained in this way.

For comparison, we also calculated the corresponding mixing energies *via* DFT for (2 × 2) ($x_{Cu} = 0.25$ and $x_{Cu} = 0.75$), ($\sqrt{3} \times \sqrt{3}$) ($x_{Cu} = 0.33$ and $x_{Cu} = 0.67$), and (2 × 1) ($x_{Cu} = 0.5$) structures. For most coverages these DFT based results are close to the corresponding points calculated by the EPI Hamiltonian for the same structures (larger circles in Fig. 3). Moreover, both the DFT calculations and the EPI Hamiltonian predict the same trends in the stabilities for all ordered structures: for the regions $x_{Cu} < 0.25$ and $x_{Cu} > 0.5$, all points lie on convex ground state lines, which implies that the corresponding distributions are stable against phase separation, while the negative curvatures around $x_{Cu} = 0.33$ indicate that coexistent $CuPd_3$(2 × 2) and CuPd(2 × 1) phases would be slightly more stable than a $CuPd_2$($\sqrt{3} \times \sqrt{3}$) phase. We had previously speculated[26] that based on the misfit between a Cu_xPd_{1-x} adlayer and Ru(0001) a composition of Cu : Pd = 24 : 76 ($x = 0.24$) might be particularly stable. The present data demonstrate that this purely geometric consideration, following Vegard's law, does not lead to a proper description of the resulting energetics, and that additional electronic effects have to be included.

At higher Cu contents, both experimental and DFT data predict a high stability of the ordered ($\sqrt{3} \times \sqrt{3}$) Cu_2Pd ground state structure which can be rationalized considering that in this phase all Pd atoms are only surrounded by Cu and that the nearest neighbor interaction potential $V(1)$ is also maximized in this composition regime (*cf*. Fig. 1). The Cu_2Pd-($\sqrt{3} \times \sqrt{3}$) phase is in fact the phase with the highest Pd content with only unlike nearest neighbors for all Pd atoms. For the (2 × 2) phase the rather low stability against separation into a Cu_2Pd ($\sqrt{3} \times \sqrt{3}$) phase coexisting with a pure Cu layer (*cf*. dotted lines in Fig. 3) is surprising, considering that this structure appears as (111) plane of the highly stable $L1_2$ type Cu_3Pd bulk alloy.[31,32,45] A similar trend has previously been reported for Cu_xPd_{1-x} surface alloys on Cu(111),[34] and was explained by the large number of possible distributions at $x_{Cu} > 0.67$, where all Pd atoms are surrounded only by Cu neighbors. Since the system Cu_xPd_{1-x} is energetically dominated by nearest-neighbor interactions (*cf*. Fig. 1 for 2D or ref. 46 for 3D), these distributions are almost degenerate.[11,34]

The remaining small discrepancies between experimentally and theoretically derived ground state energies in Fig. 3 can result from different reasons. First, a higher accuracy of the energetic description by the lattice gas Hamiltonian is likely to require the consideration of further interactions such as trio-interactions and higher, in analogy to the treatment of Cu_xPd_{1-x} bulk alloys described by Zunger *et al.*[31,32] Although, based on theoretical considerations, such multi-site interactions were considered to be small for surface alloys on a fixed substrate lattice,[11] they may still lead to small shifts in the mixing energies derived from the experimental data. Second, the actual, kinetically determined freezing temperatures in the experiments could systematically vary with coverage. Though all surfaces were annealed to the same temperature of at least 780 K, which is clearly above the freezing temperature, a concentration dependent variation of the freezing temperature between 550 and 650 K, instead of being fixed to 600 K as assumed so far, would affect the corresponding EPI values by ±10%. This, in turn, would linearly affect the calculated mixing energies. Finally, one should also consider that the differences between the EPI and DFT based mixing energies of the different structures are rather small (~10 meV per atom), which is close to the numerical uncertainty of the DFT calculations.

Formation of ordered phases

In our previous publication we tentatively explained the absence of long-range ordered phases in Cu_xPd_{1-x}/Ru(0001) surface alloys at all experimentally tested compositions by an order–disorder transition temperature T_c far below the freezing temperature of 600 K.[26] This hypothesis is supported by a simulated annealing/cool-down procedure for a monolayer Cu_2Pd/Ru(0001) surface alloy which is shown in Fig. 4b, together with representative MC generated atomic distributions at 600 K (Fig. 4a) and 1 K (Fig. 4c). The order–disorder transition T_c is reflected by the pronounced increase of the mixing enthalpy curve at around 100 K, with an uncertainty of ±30% at most due to uncertainties of the derived EPIs and in the assumed freezing temperature as discussed above. A comparably low value of T_c (100–180 K) was also reported for PdAu/Ru(0001) surface alloys.[33] The low values of T_c in surface alloys compared to their bulk analogs can be rationalized by the lower coordination of the atoms in an ordered 2D alloy compared to a bulk alloy, which reduces the energy loss associated with a defect in the ordered ground state structure, while for a comparable number of atoms the gain in configurational entropy is similar in 2D and in 3D phases.

The small driving forces for ordering in the Cu_xPd_{1-x}/Ru(0001) monolayer surface alloys and the resulting low order–disorder transition temperature provide a simple explanation for the absence of long-range ordered structures under experimentally accessible conditions. The tendency for ordering is particularly low on hexagonally packed surface alloys

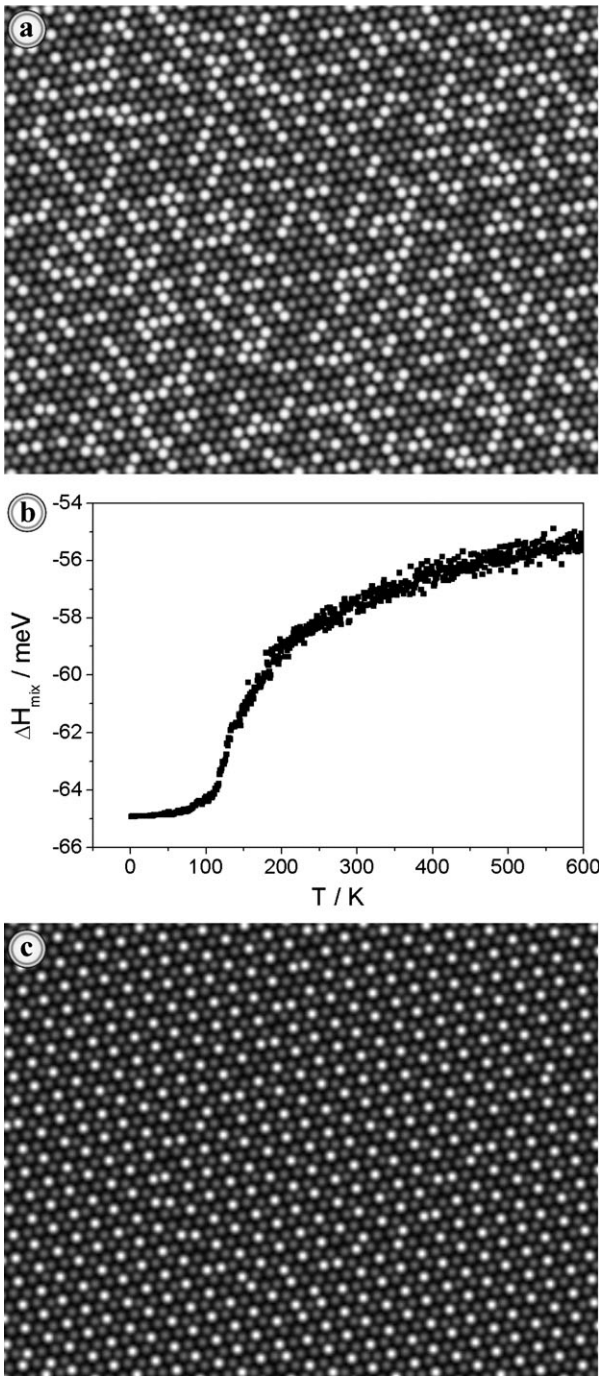

Fig. 4 Simulated annealing of a monolayer Cu_2Pd/Ru(0001) surface alloy. (a) Distribution at 600 K; (b) mixing energy as function of temperature (decreasing from 600 to 1 K); (c) distribution at 1 K.

with dominant nearest-neighbor interactions because of the relatively high degeneracy of different structures with similar compositions.[11,30] A more pronounced stabilization of ordered bimetallic surfaces with hexagonal packing can be attained on ordered bulk alloys as Pt_xSn_{1-x}, where the surface ordering is supported by the long-range order in deeper layers.

Finally, we want to briefly discuss the relevance of these findings for model studies on the catalytic properties of alloy surfaces and surface alloys. Most importantly, the catalytic properties of a given configuration do not depend on whether this represents an equilibrium configuration (at that temperature and under the respective experimental conditions) or not. It is solely determined by the structural arrangement of the components and the resulting electronic and hence chemical surface properties. If the catalytic reaction is studied at temperatures far below the onset of mixing or segregation, this reaction will therefore proceed on the frozen non-equilibrium configuration prepared before. If the reaction is investigated under conditions where the mobility of the surface region is sufficient for finally reaching the equilibrium configuration, interactions between adsorbed species and the surface have to be considered as well as they may alter the energetic situation and hence also the composition and configuration of the surface layer. This will be particularly important for alloy surfaces or multilayer surface alloys with several bimetallic layers on top of the monometallic substrate, where such interactions are likely to affect the segregation behavior and thus the composition of the catalytically accessible top layer. For monolayer surface alloys, as investigated in the present case, the latter effect is not possible, at least not for an inert substrate. In this case, the effect of the interaction with the gas phase and the adsorbed species is limited to more or less pronounced modifications of the EPIs. Finally, the interaction with adsorbed species may also alter diffusion barriers, both for lateral diffusion within the topmost layer, which in our case would affect the 2D freezing temperature, and for exchange with the substrate, which could result in additional segregation effects. Accordingly, these effects have to be tested in catalytic model studies before surface configurations produced under UHV conditions can be transferred to the reaction situation.

Hence, as long as model studies on structurally well characterized (non-equilibrium) surfaces are used to determine the adsorption or reaction behavior of specific bimetallic configurations and ensembles, the interpretation of the reaction behavior (ensemble effects, ligand effects, *etc.*) may be complicated, but is essentially straightforward. In these cases the knowledge of the interaction energies and effective pair interactions can be extremely helpful for estimating the configurations experimentally accessible and the respective preparation conditions. For adsorption or reaction on unstable surfaces, where the composition of and atomic distribution in the surface layer depend on the interaction with the adsorbed species and the gas phase, the situation is much more complex. In this case, the structure and the related energetic parameters would have to be determined *in situ*, under adsorption/reaction conditions. The pair interactions between the metal surface atoms, derived for the bare surface alloy, can provide a starting point for an estimate of the surface composition under reaction conditions, but adsorbate induced modifications and, in particular, segregation effects have to be considered as well.

4. Conclusions

The short-range order (SRO) in 2D Cu_xPd_{1-x}/Ru(0001) surface alloys, which was determined from atomically resolved STM data with chemical contrast, could be quantitatively reproduced by Monte Carlo (MC) simulations based on effective pair interactions (EPIs). For any given coverage,

the EPIs allowed us to identify the corresponding $T = 0$ ground state structures and to estimate their mixing energies, *i.e.*, the energies relative to the respective monometallic monolayer films, together with the order–disorder transition temperatures. The results derived in this way from the experimental data agree very well with corresponding DFT calculations performed for selected concentrations.

The short-range order in the Pd_xCu_{1-x} adlayer structure is dominated by effective nearest-neighbor attractions between unlike neighbors, which is reflected by a negative mixing energy in the ground state structure in both the MC based EPIs and the DFT calculations. MC simulations demonstrate, however, that none of the ordered ground state structures are stable at temperatures above 180 K, which prevents their formation at temperatures >600 K required for intermixing for kinetic reasons. Hence, the absence of a long-range order is characteristic of Cu_xPd_{1-x}/Ru(0001) surface alloys for all compositions and at all experimental conditions. Compared to bulk alloy surfaces, the driving force for surface ordering is significantly lower in surface alloys due to the lacking additional stabilization provided by interaction with a more stable long-range ordered bulk bimetallic substrate.

Acknowledgements

This work was supported by the Deutsche Forschungsgemeinschaft within the Priority Programme 1091 (Be-1201/10-1, Gr-1503/12-2)).

References

1 U. Bardi, *Rep. Prog. Phys.*, 1994, **57**, 939.
2 in *Surface Alloys and Alloy Surfaces*, ed. D. P. Woodruff, Elsevier, Amsterdam, 2002, vol. 10, in ser. *The Chemical Physics of Solid Surfaces*.
3 A. Christensen, A. V. Ruban, P. Stoltze, K. W. Jacobsen, H. L. Skriver, J. K. Nørskov and F. Besenbacher, *Phys. Rev. B: Condens. Matter Mater. Phys.*, 1997, **56**, 5822.
4 A. Groß, *Top. Catal.*, 2006, **37**, 29.
5 C. T. Campbell, *Annu. Rev. Phys. Chem.*, 1990, **41**, 775.
6 J. L. Stevens and R. Q. Hwang, *Phys. Rev. Lett.*, 1995, **74**, 2078.
7 M. Schick, G. Ceballos, T. Pelzer, J. Schäfer, G. Rangelov, J. Stober and K. Wandelt, *J. Vac. Sci. Technol., A*, 1994, **12**, 1795.
8 J. Tersoff, *Phys. Rev. Lett.*, 1995, **74**, 434.
9 G. E. Thayer, V. Ozolins, A. K. Schmid, N. C. Bartelt, M. Asta, J. J. Hoyt, S. Chiang and R. Q. Hwang, *Phys. Rev. B: Condens. Matter Mater. Phys.*, 2001, **86**, 660.
10 R. Tétot, J. Kudrnovsky, A. Pasturel, V. Drchal and P. Weinberger, *Phys. Rev. B: Condens. Matter Mater. Phys.*, 1995, **51**, 17910.
11 A. V. Ruban, H. L. Skriver, J. K. Norskov, in *Surface Alloys and Alloy Surfaces*, ed. D. P. Woodruff, Elsevier, Amsterdam, 2002, vol. 10, p. p. 1.
12 S. Müller, *J. Phys.: Condens. Matter*, 2003, **15**, R1429.
13 F. Maroun, F. Ozanam, O. M. Magnussen and R. J. Behm, *Science*, 2001, **293**, 1811.
14 M. Chen, D. Kumar, C.-W. Yi and D. W. Goodman, *Science*, 2005, **310**, 291.
15 M. Ruff, N. Takehiro, P. Liu, J. K. Nørskov and R. J. Behm, *ChemPhysChem*, in press.
16 W. M. H. Sachtler and R. A. van Santen, *Adv. Catal.*, 1977, **26**, 69.
17 W. M. H. Sachtler, in *Handbook of Heterogeneous Catalysis*, ed. G. Ertl, H. Knözinger and J. Weitkamp, VCH-Wiley, Weinheim, 1997, vol. 3, p. 1077.
18 M. Schmid, H. Stadler and P. Varga, *Phys. Rev. Lett.*, 1992, **70**, 1441.
19 F. Besenbacher, E. Laegsgaard, L. P. Nielsen, L. Ruan and I. Stensgaard, *J. Vac. Sci. Technol., B*, 1994, **12**, 1758.
20 B. Gleich, M. Ruff and R. J. Behm, *Surf. Sci.*, 1997, **386**, 48.
21 W. A. Hofer, G. Ritz, W. Hebenstreit, M. Schmid, P. Varga, J. Redinger and R. Podloucky, *Surf. Sci.*, 1998, **405**, L514.
22 F. Buatier de Mongeot, M. Scherer, B. Gleich, E. Kopatzki and R. J. Behm, *Surf. Sci.*, 1998, **411**, 249.
23 Y. Gauthier, R. Baudoing-Savois, J. M. Bugnard, W. Hebenstreit, M. Schmid and P. Varga, *Surf. Sci.*, 2000, **466**, 155.
24 T. Diemant, T. Hager, H. E. Hoster, H. Rauscher and R. J. Behm, *Surf. Sci.*, 2003, **541**, 137.
25 T. Hager, H. Rauscher and R. J. Behm, *Surf. Sci.*, 2004, **558**, 181.
26 H. E. Hoster, E. Filonenko, B. Richter and R. J. Behm, *Phys. Rev. B: Condens. Matter Mater. Phys.*, 2006, **73**, 165413.
27 S. Sakong, C. Mosch and A. Groß, *Phys. Chem. Chem. Phys.*, 2007, **9**, 2216.
28 H. Rauscher, T. Hager, T. Diemant, H. Hoster, F. Buatier de Mongeot and R. J. Behm, *Surf. Sci.*, in press.
29 Y. Gohda and Y. Groß, *J. Electroanal. Chem.,* DOI: 10.1016/j.jelechem.2006.10.015.
30 F. Ducastelle, *Order and Phase Stability in Alloys*, North Holland, Amsterdam, 1991.
31 Z. W. Lu, S. H. Wei and A. Zunger, *Phys. Rev. B: Condens. Matter Mater. Phys.*, 1992, **45**, 10314.
32 Z. W. Lu and A. Zunger, *Phys. Rev. B: Condens. Matter Mater. Phys.*, 1994, **50**, 6626.
33 B. Sadigh, M. Asta, V. Ozolins, A. K. Schmid, N. C. Bartelt, A. A. Quong and R. Q. Hwang, *Phys. Rev. Lett.*, 1999, **83**, 1379.
34 A. Bach Aaen, E. Laegsgaard, A. V. Ruban and I. Stensgaard, *Surf. Sci.*, 1997, **408**, 45.
35 N. Metropolis, A. W. Rosenbluth, M. N. Rosenbluth and A. H. Teller, *J. Chem. Phys.*, 1953, **21**, 1087.
36 K. Binder, D. M. Ceperley, J.-P. Hansen, M. H. Kalos, D. P. Landau, D. Levesque, H. Müller-Krumbhaar, D. Stauffer, J.-J. Weis, in *Monte Carlo Methods in Statiscal Physics*, ed. K. Binder, Springer-Verlag, Berlin, 1986, 2nd edn, p. 1.
37 J. N. Nelder and R. Mead, *Comput. J.*, 1965, **7**, 308.
38 W. H. Press, B. P. Flannery, S. A. Teukolsky and W. T. Vetterlin, *The Art of Scientific Computing*, Cambridge University Press, Cambridge, 1992.
39 J. M. Cowley, *J. Appl. Phys.*, 1950, **21**, 24.
40 B. E. Warren, *X-Ray diffraction*, Dover Publications Inc., New York, 1990.
41 G. Kresse and J. Furthmüller, *Phys. Rev. B: Condens. Matter Mater. Phys.*, 1996, **54**, 11169.
42 B. Hammer, L. B. Hansen and J. K. Norskov, *Phys. Rev. B: Condens. Matter Mater. Phys.*, 2007, **59**, 7413.
43 G. Kresse and D. Joubert, *Phys. Rev. B: Condens. Matter Mater. Phys.*, 2007, **59**, 1758.
44 P. Blöchl, *Phys. Rev. B: Condens. Matter Mater. Phys.*, 2007, **50**, 17953.
45 S. Takizawa, K. Terakura and T. Mohri, *Phys. Rev. B: Condens. Matter Mater. Phys.*, 1989, **39**, 5792.
46 Z. W. Lu, D. B. Laks, S. H. Wei and A. Zunger, *Phys. Rev. B: Condens. Matter Mater. Phys.*, 1994, **50**, 6642.

